

Mott-insulator phases of non-locally coupled 1D dipolar Bose gases

A. Argüelles and L. Santos

Institut für Theoretische Physik, Leibniz Universität Hannover, Appelstr. 2, D-30167, Hannover, Germany

We analyze the Mott-insulator phases of dipolar bosonic gases placed in neighboring but unconnected 1D traps. Whereas for short-range interactions the 1D systems are independent, the non-local dipole-dipole interaction induces a direct Mott-insulator to pair-superfluid transition which significantly modifies the boundaries of the lowest Mott-insulator phases. The lowest boundary of the lowest Mott regions becomes progressively constant as a function of the hopping rate, eventually inverting its slope, leading to a re-entrant configuration which is retained in 2D. We discuss the consequences of this effect on the spatial Mott-insulator plateaux in experiments with additional harmonic confinement, showing that anti-intuitively the plateaux may become wider for increasing hopping. Our results are also applicable to non-dipolar boson-boson mixtures.

Strongly-correlated atomic gases have recently attracted a rapidly-growing attention, mainly motivated by impressive developments on the manipulation of atoms in optical lattices. When loaded in these lattices, ultra cold atoms experience a periodic potential that resembles that of electrons in solids, opening fascinating links between the physics of cold atoms and solid-state physics. In particular, cold bosons restricted to the lowest lattice band can be described by the Bose-Hubbard model [1], which presents two different phases at zero temperature [2], namely a superfluid (SF) phase, and a gapped incompressible insulator phase known as Mott-insulator (MI), characterized by a commensurate occupation per lattice site. The SF to MI transition in cold bosons in optical lattices was recently observed in a remarkable experiment [3], in which the gapped nature of the MI excitation spectrum was clearly demonstrated. The realization of the MI was indeed possible due to an additional harmonic potential overimposed to the lattice that guaranteed locally the (otherwise practically impossible) commensurability condition necessary for the MI. Such inhomogeneous potential leads to the formation of spatial MI and SF shells [1, 4], which has been observed very recently [5, 6].

Among the various research lines related with optical lattices, the physics of mixtures has attracted a considerable attention. Bose-Fermi mixtures may lead to a wealth of phases of fermion composites [7], and may allow for the generation and engineering of disorder [8, 9, 10, 11]. Bose-Bose mixtures have also attracted a major interest [12, 13, 14, 15, 16]. In particular, it has been shown [13] that the interspecies interaction may lead to the formation of a pair superfluid (PSF), i.e. a superfluid of boson-boson (or hole-hole) composites, which occurs in addition to MI phases for both components, as well as uncorrelated superfluid phases in each one of the components (2SF).

Dipolar gases also attract currently a major interest, motivated by recent experiments on atoms with large magnetic moment [17], polar molecules [18] and Rydberg atoms [19]. In these gases the long-range and anisotropic dipole-dipole interactions (DDI) become sig-

nificant or even dominant when compared to the short-range isotropic interactions [20]. The DDI can play an important role in the physics of lattice bosons, leading to additional phases, as checker-board or supersolid, which may be easily controllable by manipulating the atomic confinement [21]. In addition, contrary to short-range interacting gases for which disconnected sites (i.e. without hopping between them) are fully independent, the long-range character of the DDI induces a coupling even for unconnected sites. The latter leads to fundamentally new physics, as e.g. a condensate of filaments [22] or inelastic interlayer scattering for dipolar solitons [23].

In this Letter, we show that the non-local DDI induces a direct MI-to-PSF transition for neighboring unconnected 1D dipolar gases, which significantly modifies the boundaries of the lowest 1D MI phases. The same effect is also expected under appropriate conditions for non-dipolar boson-boson mixtures. Remarkably, the lowest boundary of the first MI lobes eventually inverts its slope as a function of the hopping rate, leading to a re-entrant scenario, which is maintained in 2D. We show that this effect has direct consequences on the spatial extension of the MI plateaux for the case of an overimposed harmonic confinement. Anti-intuitively, we show that the plateaux extension may become constant or even wider for increasing hopping.

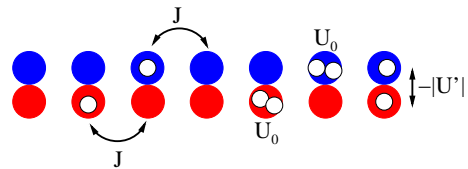


Figure 1: Scheme of the system considered in this Letter.

In the following, we consider dipolar bosons placed at two neighboring, but disconnected, 1D traps (wires), which can be created using micro-magnetic confinement [24] or sufficiently strong 2D optical lattices. In the latter case, the required two-site configuration may be generated by super-lattice techniques or by selectively empty-

ing 1D sites neighboring the desired pair. Along the 1D systems we assume an additional lattice equal for both 1D traps, which leads to the ladder configuration shown in Fig. 1. In the following we borrow from the literature on spin ladders the terms leg (each wire) and rung (pair of neighboring sites belonging to different legs). In this Letter, we are mostly concerned about interlayer effects, and hence we consider a configuration for which only the (attractive) DDI between sites at the same rung plays a significant role. This is the case, if the dipoles are oriented forming an angle φ with the axis of the wires, such that $\cos^2 \varphi = 1/3$. In that case, the DDI between neighbors at the same leg vanishes, whereas the DDI between sites in the same rung is attractive. There is in principle an additional non zero diagonal DDI between sites in neighboring rungs belonging to different legs. These terms can be made negligible by considering the spacing between rungs, $\gamma > 1$ times larger than the separation between the two legs. In that case the spurious diagonal interaction is a factor $(1 + 2\sqrt{2}\gamma)/(1 + \gamma^2)^{5/2}$ ($\simeq 0.03$ for $\gamma = 3$) smaller than that between sites in the same rung. Of course, for other dipole and lattice configurations, the DDI between sites belonging to the same leg cannot be neglected, and interesting physics can be expected [25] and will be studied elsewhere.

Under the previous conditions the system is described by a Bose-Hubbard Hamiltonian (BHH) of the form

$$\begin{aligned} \hat{H} = & -J \sum_{\alpha=1,2} \sum_{\langle i,j \rangle} \{ \hat{b}_i^{(\alpha)\dagger} \hat{b}_j^{(\alpha)} + H.c. \} \\ & + \frac{U_0}{2} \sum_{\alpha=1,2} \sum_i \hat{n}_i^{(\alpha)} (\hat{n}_i^{(\alpha)} - 1) \\ & - |U'| \sum_i \hat{n}_i^{(1)} \hat{n}_i^{(2)} - \mu \sum_{\alpha=1,2} \hat{n}_i^{(\alpha)}, \end{aligned} \quad (1)$$

where $\hat{b}_i^{(\alpha)}$, $\hat{b}_i^{(\alpha)\dagger}$, and $\hat{n}_i^{(\alpha)}$ are, respectively, the annihilation, creation, and number operators for the site i at the leg α . J describes the hopping between neighboring sites i and j in each leg, U_0 the on-site interactions (a combination of short-range and dipolar contributions [21]), and we consider the same chemical potential μ in both legs. Atoms in sites at the same rung interact attractively by the DDI, which is characterized by a coupling $-|U'|$.

In the following we analyze the effects of the coupling U' in the physics of the MI phases for the 1D wires. Note that the Hamiltonian (1) is formally equivalent to the case of two bosonic species in a 1D array, with equal chemical potential μ for both, equal hopping J , equal on-site intra-species interactions U_0 , and an interspecies interaction $-|U'|$. Hence, our results can be equally applied to boson-boson mixtures under these constraints. Indeed, as we show below, the PSF phase introduced in the context of Boson-Boson mixtures [13] is crucial for the understanding of the physics discussed below.

In our analysis of the ground states of \hat{H} , we have employed Matrix-Product-State (MPS) techniques, follow-

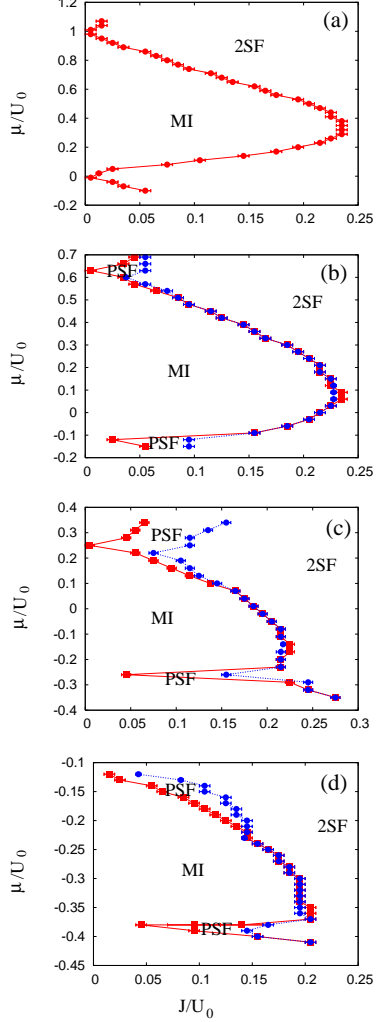


Figure 2: MI lobes as a function of J/U_0 and μ/U_0 , for $|U'|/U_0 = 0$ (a), 0.25 (b), 0.5 (c) and 0.75. The calculations were made for $L = 12$ and $D = 5$. The error bars indicate the change in the order parameters, (\blacksquare) Ψ_{PSF} and (\bullet) $\langle b \rangle$, from $< 10^{-4}$ to $> 10^{-2}$.

ing closely the method of Ref. [26]. The MPS represent an optimal Ansatz [27] for problems as that of this Letter. Adapted to the two-leg problem, with L sites per leg, the MPS Ansatz for the many-body wavefunction is:

$$|\Psi\rangle = \sum_{\{n_i^{(\alpha)}=0\}}^{n_{max}} A_{[1]}^{[n_1^{(1)}, n_1^{(2)}]} \dots A_{[L]}^{[n_L^{(1)}, n_L^{(2)}]} |\{n_i^{(\alpha)}\}\rangle, \quad (2)$$

where we consider a maximal number of atoms n_{max} per site, and $A_{[j]}^{[n_j^{(1)}, n_j^{(2)}]}$ is a $D \times D$ matrix, associated to the case of $n_j^{(1)}$ and $n_j^{(2)}$ atoms at the site j of both legs. In the following we focus on the regime of low average occupation per site around the first MI lobe, and hence in our calculations it proves enough $n_{max} = 2$. In addition, we have checked in our calculations that relatively low ma-

trix dimensions $D = 6$ describe properly the problem under consideration. The MPS Ansatz enormously simplify the original problem (which scales exponentially with L), since it has a complexity given by $(n_{\max} + 1)D^2L$. Using a similar approach as that of Ref. [26] we developed a numerical algorithm that allows us to recursively adapt the matrices until reaching the ground state. This method resembles in many ways that of finite-size Density-Matrix-Renormalization-Group techniques [28].

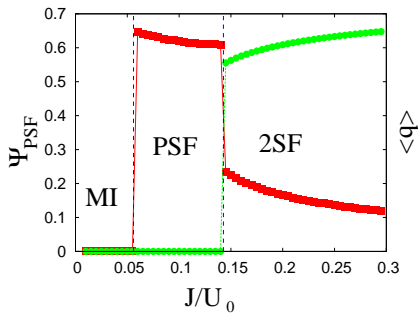


Figure 3: (■) ψ_{PSF} and (●) $\langle b \rangle$ as a function of J/U_0 for $\mu = -0.15$ and $|U'|/U_0 = 0.75$ with $L = 24$ and $D = 6$.

Fig. 2 shows the results of our simulations for the surroundings of the lowest MI lobe (with $\langle n_i^{1,2} \rangle = 1$) for $|U'|/U_0 = 0$ (a), $1/4$ (b), $1/2$ (c) and $3/4$ (d). Note that in order to avoid collapse in a single site, $|U'| < U_0$. For the case of $U' = 0$, the usual Mott-lobes are recovered [29]. However, the dependence of the lobe boundaries in the μ - J phase space changes significantly when $|U'|$ grows. Note, in particular, that the lowest boundary becomes progressively flatter when $|U'|$ approaches $U_0/2$. Indeed our analytical calculations (see below) show that for $|U'| > U_0/2$ the slope of the lowest boundary of the MI lobe inverts its sign. This behavior is however difficult to observe in our numerical calculations due to the very narrow region between the MI-lobe and the region of zero occupation. In the following we discuss in more detail the physics behind the distortion of the MI lobes, and the implications of this distortion on the spatial extension of the MI lobes in axially trapped gases.

The boundaries of the MI lobes are provided by the energy gap between the MI state and the lowest excited state conserving the particle number. In usual (single-component) BHH [2] this lowest excitation is provided by particle-hole excitations. The MI boundaries can then be calculated by a strong-coupling expansion (SCE) [30], estimating the energy of a state with an extra particle and a state with an extra hole. This is indeed the case of $U' = 0$, where the lowest excitations are given by uncorrelated particle-hole excitations in both wires. The situation changes for $|U'| > 0$, since for sufficiently low tunneling, there is a direct transition between MI and PSF phases, i.e. superfluid phases of composites (or composite holes) [13]. In that case the first excitation of the

MI lobe is given by the correlated creation of pairs of particles (or holes) at opposite sites of the two wires, explaining the qualitative change in the shape of the lobe boundaries. In particular, a second-order SCE in $J/|U'|$ [31], provides the following dependence for sufficiently low tunneling for the lowest boundary of the MI lobe with n_0 particles per site:

$$\frac{\mu}{U_0} = n_0 - 1 + \frac{|U'|}{U_0} \left(\frac{1}{2} - n_0 \right) - 4 \left(\frac{J}{U_0} \right)^2 \left[n_0(n_0 + 1) - \frac{(n_0^2 - 1)/2}{2 - |U'|/U_0} - \frac{n_0^2 U_0}{|U'|} \right] \quad (3)$$

From (3) it becomes clear that for any $U' > 0$ the gap boundaries are quadratic (and not linear) in J for sufficiently low J . Interestingly, the lowest boundary of the first MI region ($n_0 = 1$) inverts its slope at $J = 0$ for $|U'| > U_0/2$, in agreement with our numerical results. One may also observe that an inversion of the slope of the lowest boundary is expected also for $n_0 = 2$ at $|U'|/U_0 \simeq 0.85$, but it is not expected for $n_0 > 2$.

In our numerical simulations, we revealed the presence of the pairing-phases by monitoring $\Psi_{PSF} = |\langle \hat{b}^{(1)} \hat{b}^{(2)} \rangle - \langle \hat{b}^{(1)} \rangle \langle \hat{b}^{(2)} \rangle|$ [32]. A typical dependence of Ψ_{PSF} and $\langle b \rangle = \langle b^{(1,2)} \rangle$ in our simulations is depicted in Fig. 3 for a fixed chemical potential. The MI region is characterized as that in which both $\Psi_{PSF} = \langle b \rangle = 0$. We denote the PSF region as that in which $\Psi_{PSF} \neq 0$ but $\langle b \rangle = 0$. Finally the 2SF region is that in which $\langle b \rangle \neq 0$. Note that there is a finite coexistence region in which both $\Psi_{PSF} \neq 0$ and $\langle b \rangle \neq 0$. Repeating the calculations for different chemical potentials we obtain the results depicted in Figs. 2. Note that, as we mentioned above, a direct MI-PSF transition can be observed in Figs. 2 at low J/U_0 , which results in a clear distortion of the MI boundaries when compared to the $U' = 0$ case.

The qualitative change in the shape of the MI lobe has important consequences on the spatial extension of the MI and SF regions in the presence of an overimposed harmonic confinement. In order to analyze this point, we consider a harmonic trap along the wires, such that a term $\Omega \sum_{i,\alpha} i^2 \hat{n}_i^{(\alpha)}$ is added to the BHH. This term induces a local chemical potential $\mu_i = \mu_0 - \Omega i^2$, where μ_0 is the local chemical potential at the trap center. Hence, μ_i scans values $\mu < \mu_0$. If for a given tunneling rate, the system with μ_0 is inside the first MI lobe, it is hence expected the appearance of a MI shell at the trap center, characterized by a plateau in the average population per site ($\langle n \rangle = 1$), surrounded by a second SF shell (with $\langle n \rangle < 1$) [1, 4]. For $U' = 0$, for a fixed chemical potential, it is intuitively expected that the MI plateau shrinks when J/U_0 increases, until eventually disappear. Indeed, this is the case, since the lowest boundary of the MI lobe increases with J , hence decreasing the spatial MI region (Fig. 4(a)). However, when $|U'|$ grows, the change in the slope of the lowest boundary of the first

MI lobe leads to a significant modification of the spatial extension of the MI plateau. In particular, as shown in Figs. 4, the basically J -independent lowest MI boundary for $|U'| = U_0/2$ leads to a J -independent MI plateau (Fig. 4(c)). Moreover, for $|U'| > U_0/2$, the re-entrant character of the MI lobe leads to the anti-intuitive observation, that for enhanced mobility (J larger) the MI plateaux become even broader (Fig. 4(d)).

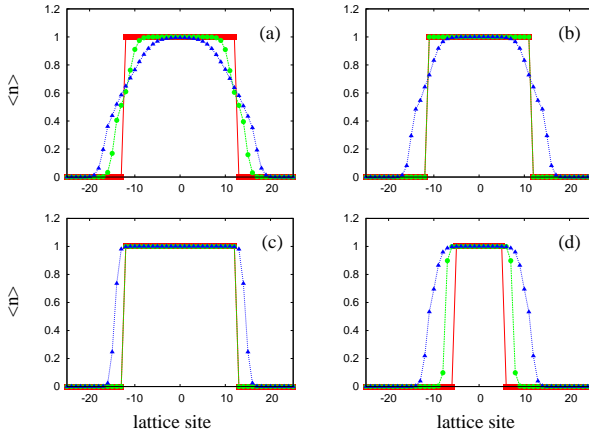


Figure 4: Spatial distribution of $\langle n \rangle$ for $U'/U_0 = 0$ (a), 0.25 (b), 0.5 (c) and 0.75 (d), for, respectively $10^4\Omega/U_0 = 12.3, 9.26, 9.26, 4.32$ for $J/U_0 = 0$ (■), 0.05 (●), 0.1 (▲).

Although a detailed 2D analysis is beyond the scope of this Letter, and will be the subject of further investigations, we stress here that the SCE for 2D lattices at unconnected layers (or equivalently to two-component bosonic gases in 2D lattices) shows that the lowest boundary of the first MI lobe follows at low J the relation (3) but substituting $2(J/U_0)^2$ by $z(J/U_0)^2$, where z is the coordination number. Hence, the change in the sign of the slope occurs exactly as for 1D, and thus a re-entrant scenario is also expected in 2D.

In this Letter we have analyzed the physics of dipolar gases in unconnected neighboring 1D systems. Whereas without dipolar interactions the 1D systems are independent, the nonlocal dipole-induced interlayer interaction leads to a direct MI to PSF transition, significantly distorting the MI-lobes along the wires. In particular, the lowest boundary of the first MI lobes becomes progressively flatter as a function of the hopping, inverting eventually its slope, leading to a re-entrant configuration (that remains in 2D). We have shown that such an effect leads to a non-trivial behavior of the MI plateaux in experiments with an axial harmonic confinement [5, 6]. In particular, the MI plateaux may (for low hopping) become insensitive to the hopping, or even anti-intuitively grow for larger tunneling. Finally, we would like to stress that our results also apply to two-component Bose gases, predicting exciting phenomenology in on-going experiments in bosonic mixtures in lattices.

Conversations with M. Lewenstein, S. Weßel, and T. Vekua are acknowledged. We thank J. I. Cirac, S. Manmana, K. Rodríguez, S. Weßel, and very especially J. J. García -Ripoll for their support concerning the numerical simulations. This work was supported by the DFG (SFB-TR21, SFB407, SPP1116).

- [1] D. Jaksch *et al.*, Phys. Rev. Lett. **81**, 3108 (1998).
- [2] M. P. A. Fisher *et al.*, Phys. Rev. B **40**, 546 (1989).
- [3] M. Greiner *et al.*, Nature **415**, 39 (2002).
- [4] G. G. Batrouni *et al.*, Phys. Rev. Lett. **89**, 117203 (2002).
- [5] S. Foelling, cond-mat/0606592.
- [6] G. K. Campbell *et al.*, cond-mat/0608370.
- [7] M. Lewenstein *et al.*, Phys. Rev. Lett. **92**, 050401 (2004).
- [8] A. Sanpera, *et al.*, Phys. Rev. Lett. **93**, 040401 (2004).
- [9] U. Gavish and Y. Castin, Phys. Rev. Lett. **95**, 020401 (2005).
- [10] K. Günter *et al.*, Phys. Rev. Lett. **96**, 180402 (2006).
- [11] S. Ospelkaus *et al.*, Phys. Rev. Lett. **96**, 180403 (2006).
- [12] E. Altman *et al.*, New J. Phys. **5**, 113 (2003).
- [13] A. Kuklov, N. Prokof'ev, and B. Svistunov Phys. Rev. Lett. **92**, 050402 (2004).
- [14] K. Ziegler, Phys. Rev. A **68**, 053602 (2003).
- [15] L. Mathey, cond-mat/0602616.
- [16] T. Mishra, R. V. Pai, and B. P. Das, cond-mat/0610121.
- [17] A. Griesmaier *et al.*, Phys. Rev. Lett. **94**, 160401 (2005).
- [18] H.-L. Bethel and G. Meijer, Int. Rev. Phys. Chem. **22**, 73 (2003).
- [19] D. Tong *et al.*, Phys. Rev. Lett. **93**, 063001 (2004).
- [20] S. Yi and L. You, Phys. Rev. A **61**, 041604 (2000); K. Góral, K. Rzżewski, and T. Pfau, Phys. Rev. A **61**, 051601 (2000); L. Santos *et al.*, Phys. Rev. Lett. **85**, 1791 (2000).
- [21] K. Góral, L. Santos, and M. Lewenstein, Phys. Rev. Lett. **88**, 170406 (2002).
- [22] D.-W. Wang, M. D. Lukin and E. Demler, Phys. Rev. Lett. **97**, 180413 (2006).
- [23] R. Nath, P. Pedri and L. Santos, cond-mat/0610703.
- [24] S. Wildermuth *et al.*, Nature **435**, 440 (2005).
- [25] T. Vekua, private communication.
- [26] F. Verstraete, J. J. Garcia-Ripoll, J. I. Cirac, Phys. Rev. Lett. **93**, 207204 (2004).
- [27] F. Verstraete and J.I. Cirac, Phys. Rev. B **73**, 094423 (2006).
- [28] R. M. Noack and S. R. Manmana, AIP Conf. Proc. **789**, 93 (2005).
- [29] Some features at the lobe tip are not fully recovered due to finite-size effects.
- [30] J. K. Freericks and H. Monien, Phys. Rev. B **53**, 2691 (1996).
- [31] Note that the SCE is worse when U' decreases.
- [32] Strictly speaking this order parameter should vanish in the thermodynamic limit, since we are working in 1D. However, due to finite size, it acquires a finite nonzero value, being zero both in the MI phase and for uncorrelated pairs and holes in the two wires, and it is in this sense useful to characterize the appearance of the pairing phases in our calculations.